

Supplementary data

One-pot direct conversion of levulinic acid into high-yield valeric acid over a highly stable bimetallic Nb-Cu/Zr-doped porous silica catalyst

Neha Karanwal,^a Deepak Verma,^{a,b,c} Paresh Butolia,^c Seung Min Kim,^d Jaehoon Kim^{*,a,b,c}

^aSKKU Advanced Institute of Nanotechnology (SAINT), Sungkyunkwan University,
2066 Seobu-Ro, Jangan-Gu, Suwon, Gyeong Gi-Do 16419, Republic of Korea

^bSchool of Mechanical Engineering, Sungkyunkwan University,
2066 Seobu-Ro, Jangan-Gu, Suwon, Gyeong Gi-Do 16419, Republic of Korea

^cSchool of Chemical Engineering, Sungkyunkwan University,
2066 Seobu-Ro, Jangan-Gu, Suwon, Gyeong Gi-Do 16419, Republic of Korea

^dInstitute of Advanced Composite Materials, Korea Institute of Science and Technology,
Chudong-ro 92, Bongdong-eup, Wanju-gun, Jeonranbuk-do, 55324, Republic of Korea

*Corresponding author, *E-mail:* jaehoonkim@skku

Table S1 Comparison of yields and selectivities in the formation of valeric acid from various feedstocks using noble and non-noble metal-based catalysts

Catalyst	Reaction conditions			Solvent	Catalyst -to-feed ratio	Conv. (%)	VA yield (%)	VE yield (%)	VA+VE ^a yield (%)	References
	H ₂ (MPa)	T (°C)	t (h)							
Noble metal-based catalysts										
Ru/HZSM-5	4	200	4	Dioxane	1:8	90	26.9	18.9	45.8	Luo <i>et al.</i> , J. Catal., 2013 ¹
Ru/SBA-SO ₃ H	4	240	6	Ethanol	1:2.3	100	N.A. ^b	N.A.	90.0	Pan <i>et al.</i> , Green Chem., 2013 ²
Ru/HZSM-5	4	200	10	Dioxane	1:10	100	66.3	25.0	91.3	Luo <i>et al.</i> , J. Catal., 2014 ³
Pt/HMFI ^c	0.8	200	6	Solvent-free	1:2	100	99	0	99	Kon <i>et al.</i> , Catal. Sci. Tech., 2014 ⁴
Pt/HMFI ^c	0.8	200	3	Methanol	1:2	N.A.	N.A.	87	N.A.	
Pd/C+Hf(OTf) ₄	5	150	6	Octane	1:10+2.5	99	92	0	92	Zhou <i>et al.</i> , Green Chem., 2018 ⁵
Pd/AlMCM-41	6	270	10	Octane	1:3	>99	45	0	45	Wang <i>et al.</i> , Chemistry Select, 2018 ⁶
Pt/HZSM-5	1	200	5	Water	1:12	100	91.4	0	91.4	Xiao-min <i>et al.</i> , J. Fuel Chem. Technol., 2017 ⁷
Pt/TiO ₂ , Pd/TiO ₂ ,	1–4	200–300	100	Gas phase	-	65.0	N.A.	20–50	N.A.	Lange <i>et al.</i> , Angew. Chem., Int. Ed., 2010 ⁸
Non-noble metal-based catalysts										
Co@HZSM-5	3	240	3	EtOH	1:10	100	23	74	97	Sun <i>et al.</i> , ACS Catal. 2014 ⁹
Ni/K _{0.5} /HZSM-5	3	240	2.96 h ^{-1,d}	EtOH	-	100	N.A.	N.A.	90	Sun <i>et al.</i> , Appl. Cat. B, 2016 ¹⁰
W-Ni/TiO ₂	0.1	270	4.6 mL s ⁻¹ g _{cat} ^{-1,e}	Water	-	74	36	0	36	Kumar <i>et al.</i> , Appl. Cat. A, 2017 ¹¹
Ni-W/HZSM5	0.1	270	9.7 mL s ⁻¹ g _{cat} ^{-1,e}	Water	-	40	26	0	26	Velisoju <i>et al.</i> , Appl. Catal. A, 2018 ¹²
Nb-Cu/ZPS	3	150	2	Water	1:8	96	92.5	0	93	This work
					1:4	100	99.8	0	99.8	

^aVA = valeric acid; VE = valeric acid alkyl esters (methyl valerate and ethyl valerate); ^bN.A. = Not available; ^cHMFI = Commercial H⁺-type MFI zeolite (HMFI) with a SiO₂/Al₂O₃ ratio of 22.3; ^dThree-step reaction; ^eWeight hour space velocity

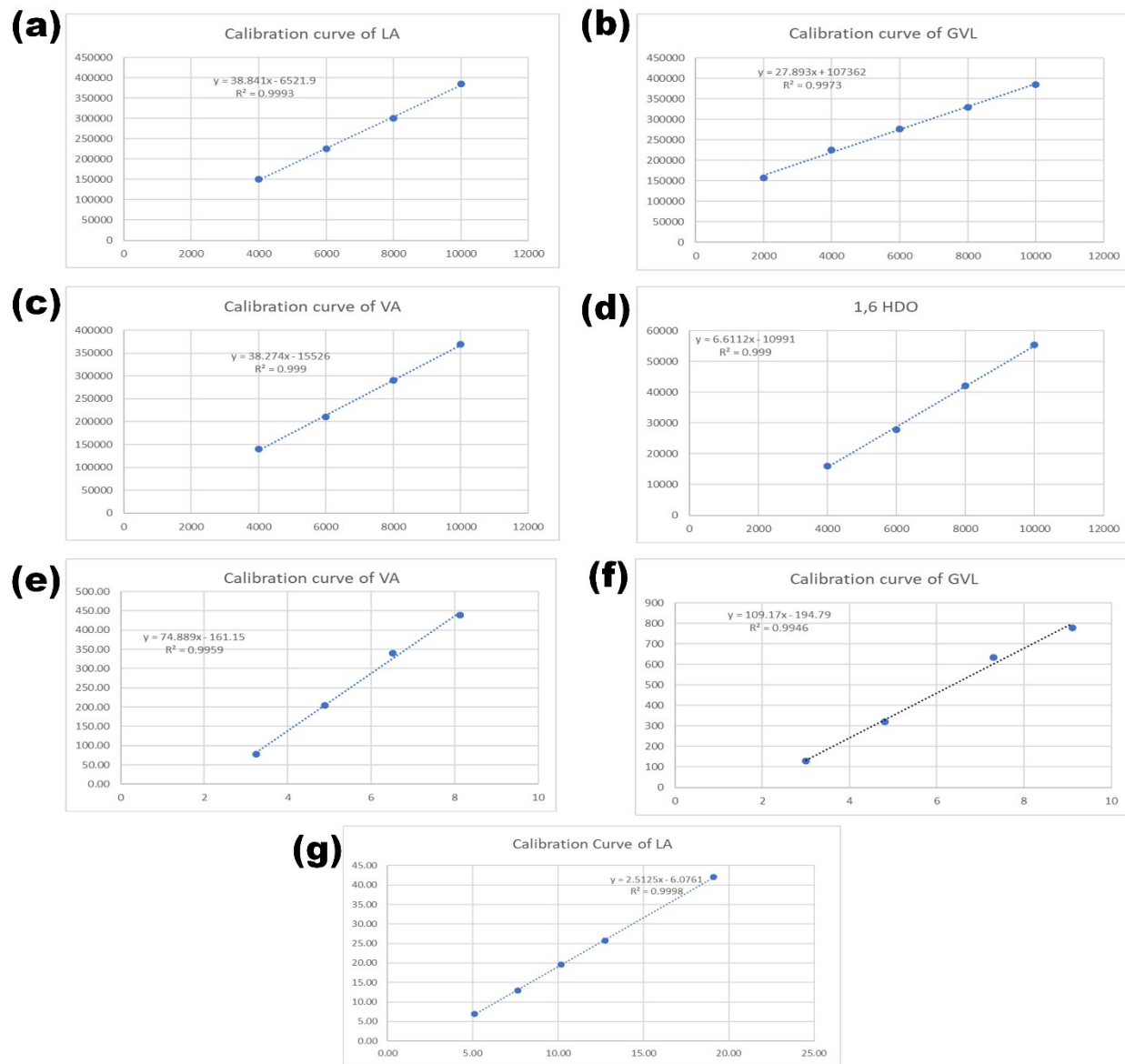


Fig. S1 Calibration curves for quantification of (a) LA by HPLC, (b) GVL by HPLC, (c) VA by HPLC, (d) 1,6-hexanediol (as an internal standard) by HPLC, (e) VA by GC-FID, (f) GVL by GC-FID, and (g) LA by GC-FID.

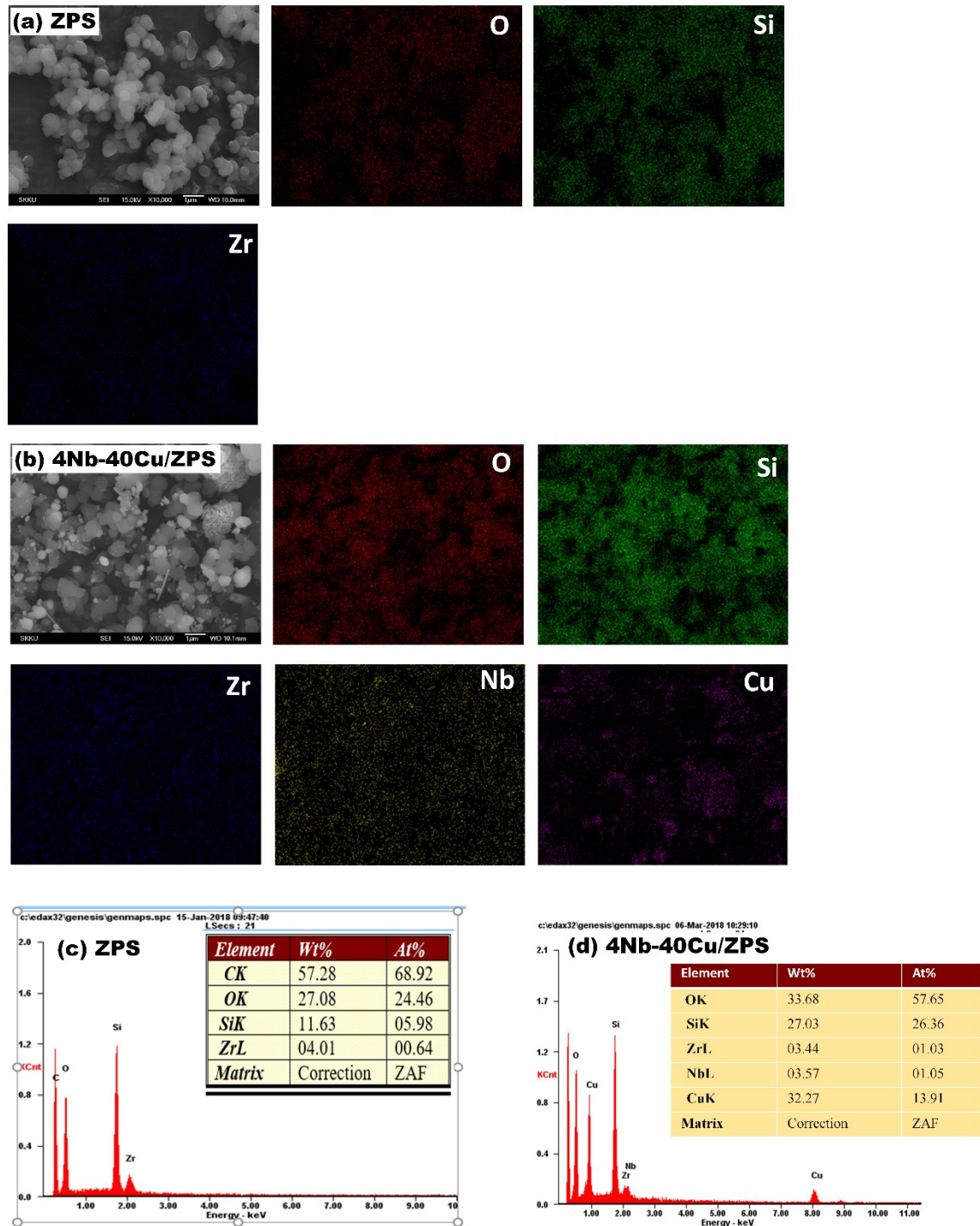


Fig. S2 SEM images and EDS mapping of (a) ZPS and (b) 4Nb-40Cu/ZPS. Chemical composition of (c) ZPS and (d) 4Nb-40Cu/ZPS.

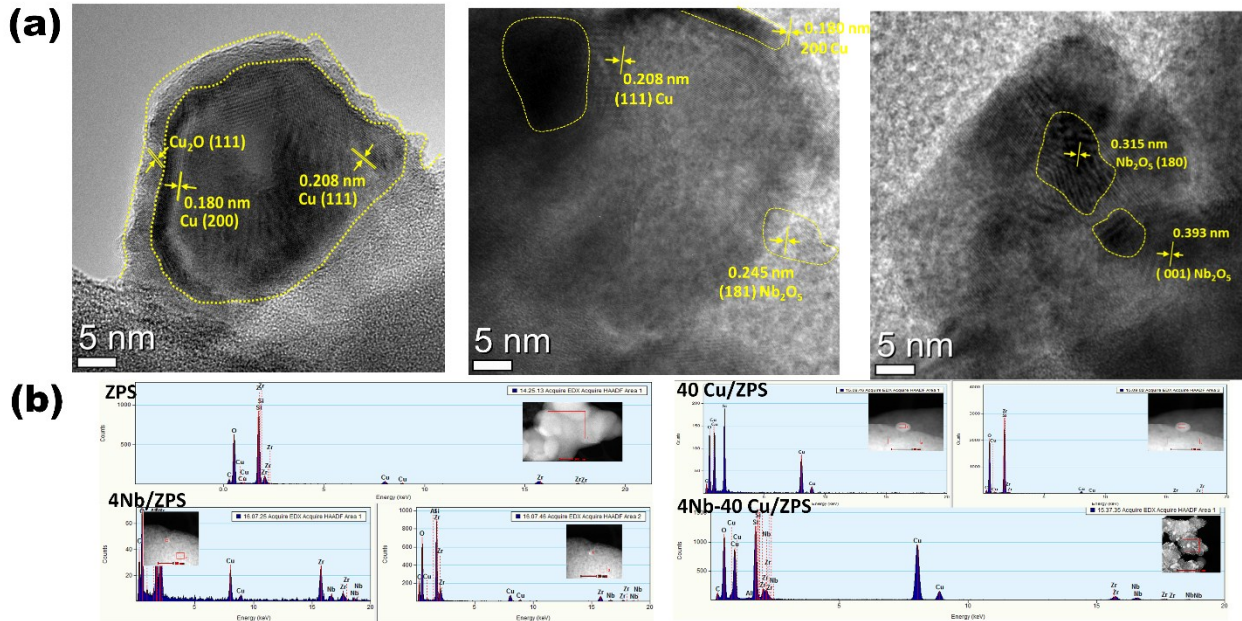


Fig. S3 (a) HR-TEM images of 4Nb-40Cu/ZPS and (b) EDX data of HAADF-STEM images of ZPS, 2Nb/ZPS, 40Cu/ZPS and 4Nb-40Cu/ZPS. Cu was shown in the EDX data of ZPS because of the Cu grid.

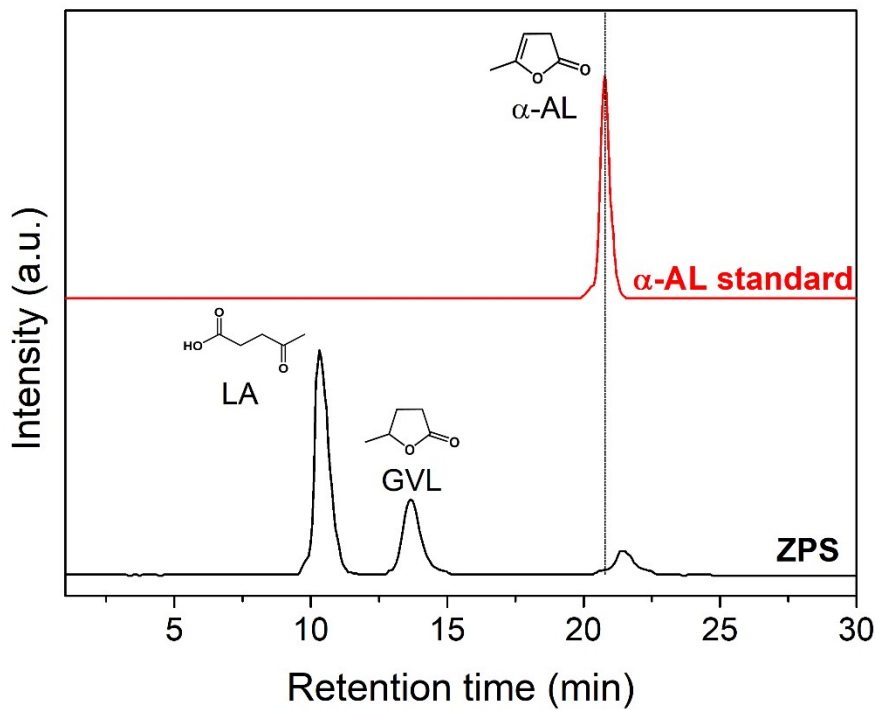


Fig. S4 HPLC profiles of the reaction products formed in the presence of ZPS and α -angelica lactone (α -AL standard). Reaction conditions: 3.4 mmol of levulinic acid (LA), 0.05 g of catalyst, 30 mL of H_2O , 150 °C, initial H_2 pressure of 3 MPa, 2 h. GVL: γ -valerolactone.

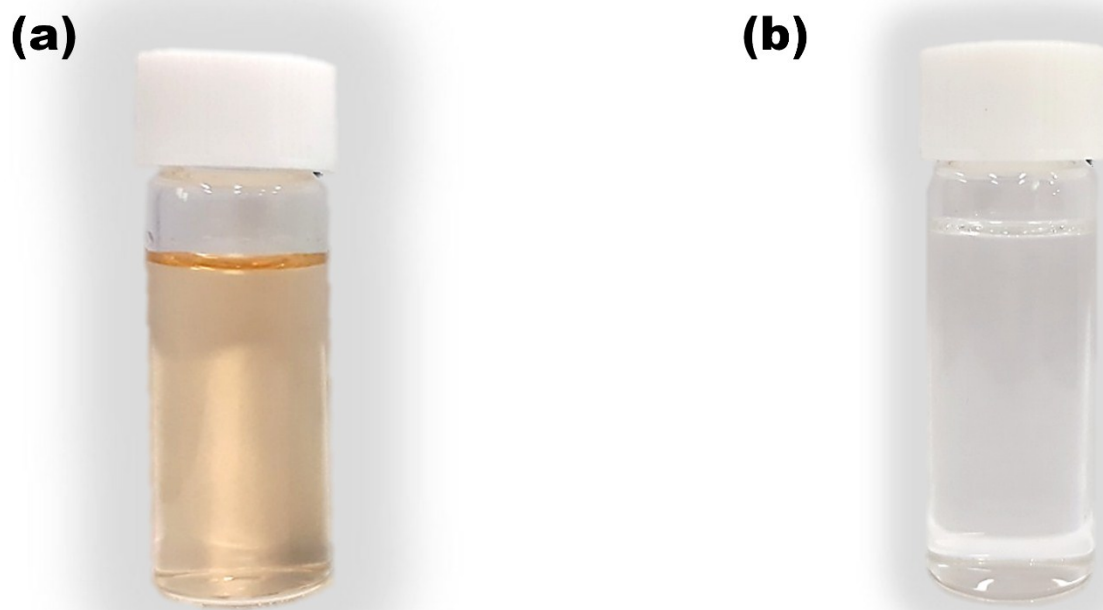


Fig. S5 Color of liquid produced from the conversion of LA over (a) 40Cu/ZPS and (b) 4Nb-40Cu/ZPS. Reaction conditions: 3.4 mmol LA, 0.05 g of catalyst, 30 mL H₂O, 150 °C, 3 MPa initial H₂ pressure, 2 h.

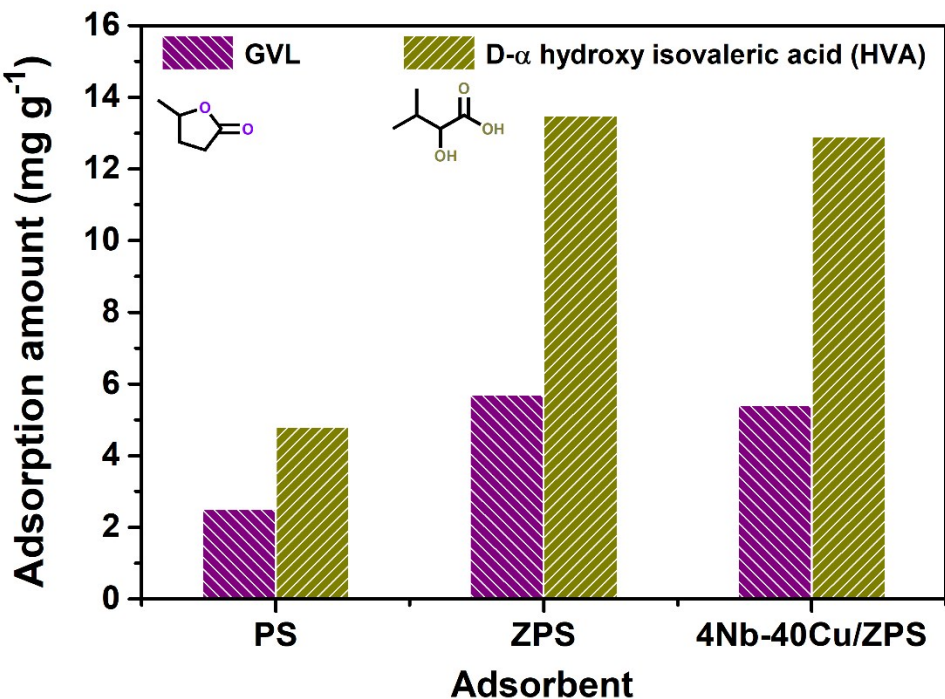


Fig. S6 Adsorption of GVL and D- α hydroxy isovaleric acid in water over PS, ZPS, and the 4Nb-40Cu/ZPS catalysts.

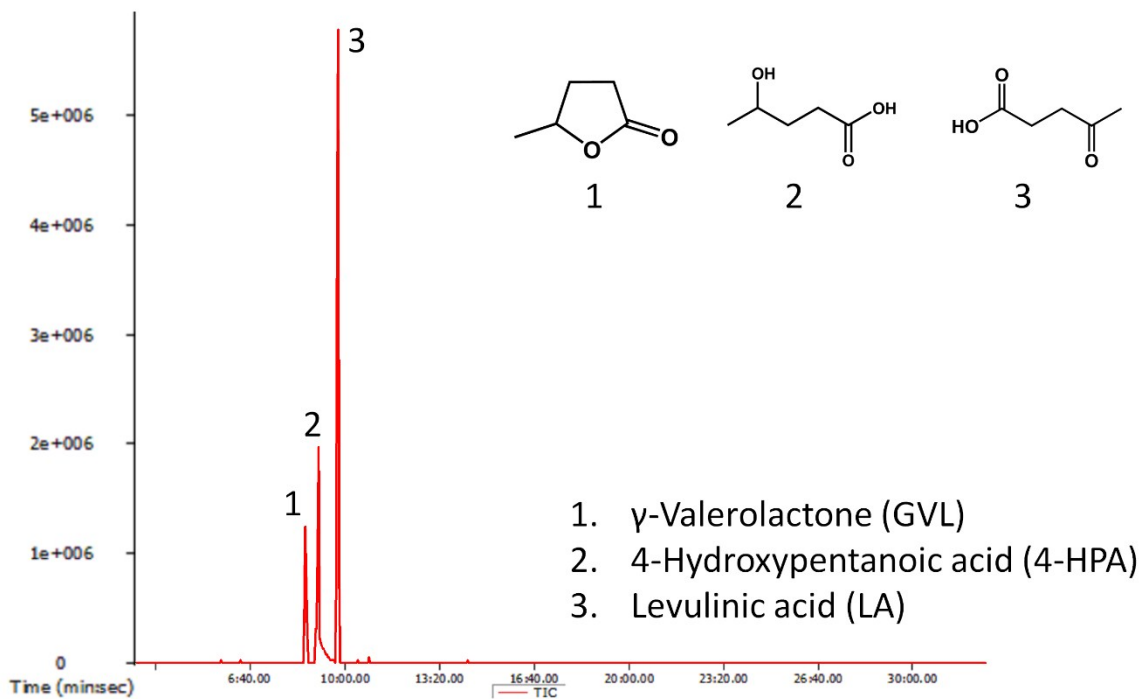


Fig. S7 GC-TOF/MS chromatogram of reaction mixture produced using 3.4 mmol of LA, 0.05 g of 40Cu/ZPS, 30 mL of H₂O, 100 °C, initial H₂ pressure of 1 MPa, and reaction time of 1 h.

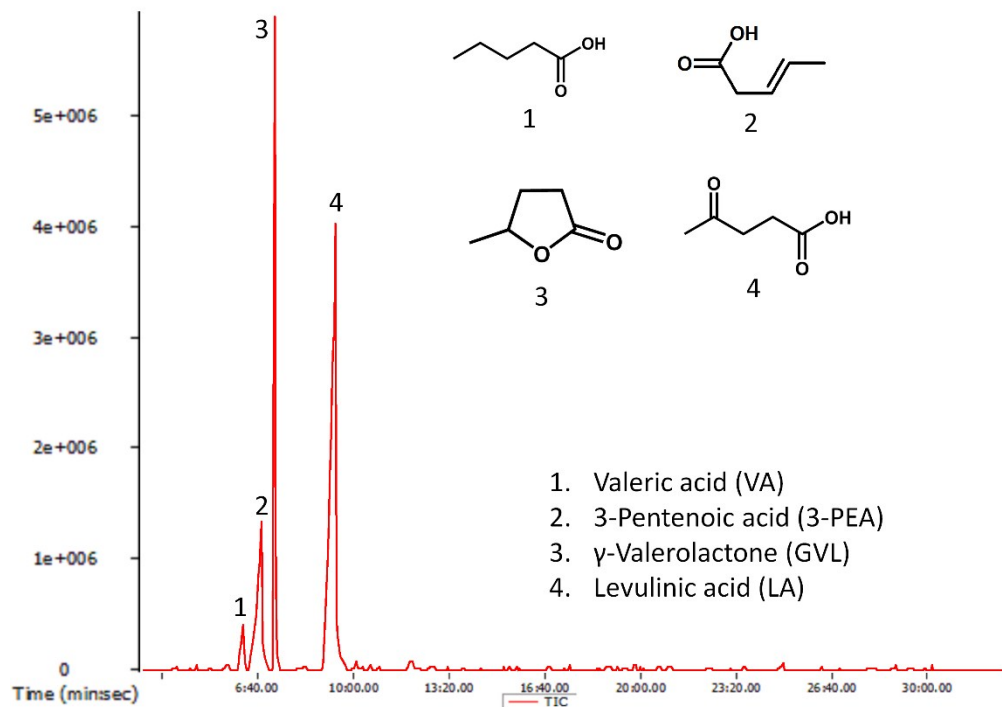
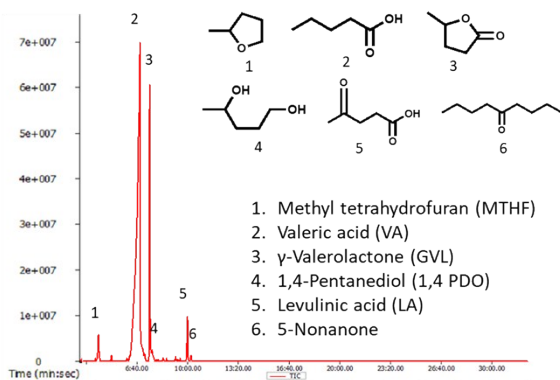
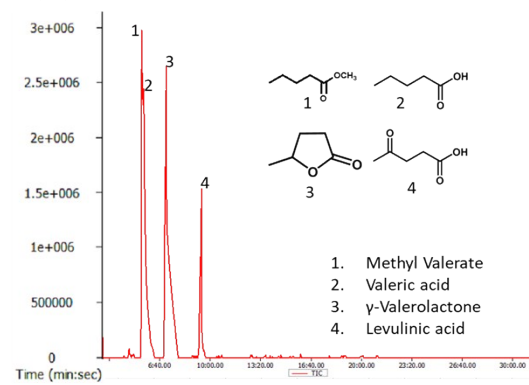


Fig. S8 GC-TOF/MS profiles of reaction mixtures produced over bimetallic 4Nb-40Cu/ZPS catalysts. Reaction conditions: 3.4 mmol LA, 30 mL H₂O, 120 °C, 1.5 MPa initial H₂ pressure, 1 h.

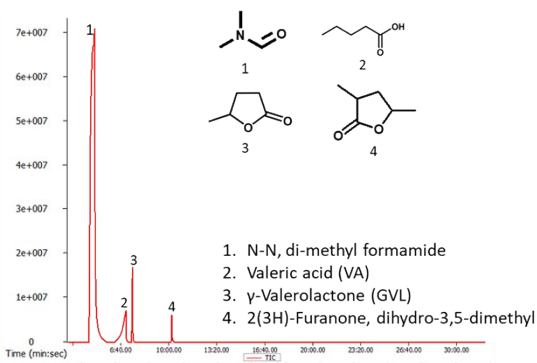
(a) THF



(b) Methanol



(c) DMF



(d) Hexane

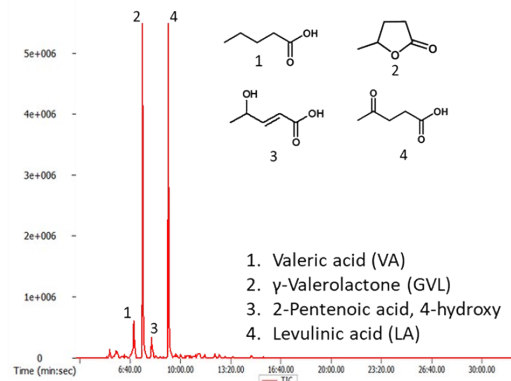


Fig. S9 GC-TOF/MS chromatograms of reaction mixtures produced over bimetallic 4Nb-40Cu/ZPS catalysts. Reaction conditions: 3.4 mmol LA, 30 mL solvent, 3.0 MPa initial H₂ pressure, 2 h.

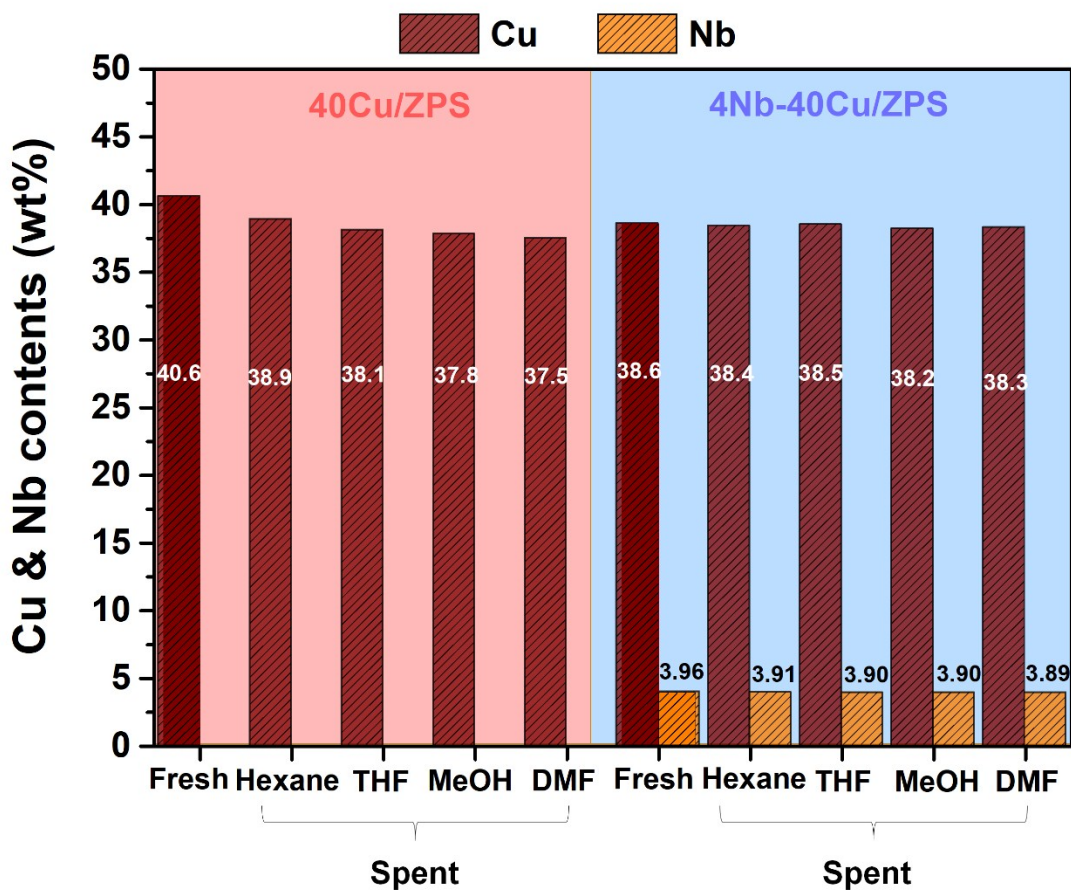


Fig. S10 Cu and Nb content of fresh and spent 40Cu/ZPS and 4Nb-40Cu/ZPS catalysts after 1st run in various organic solvents. Reaction conditions: 3.4 mmol LA, 0.05 g catalyst, 40 mL solvent, 150 °C, 3 MPa initial H₂ pressure, 2 h.

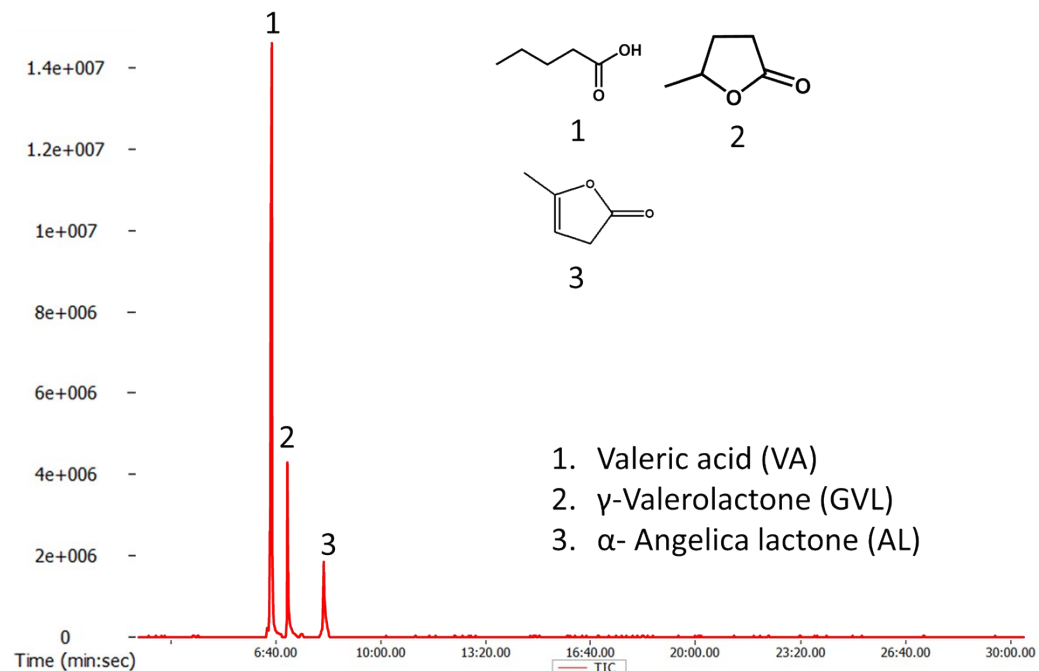


Fig. S11 GC-TOF/MS chromatograms of reaction mixtures produced over 4Nb-40Cu/ZPS catalyst in the conversion of α -AL. Reaction conditions: 3.4 mmol α -AL, 0.05 g catalyst, 40 mL H₂O, 120 °C, 3 MPa initial H₂ pressure, 2 h.

Conversion of LA and valeric acid to valerate esters

As discussed in the Introduction, valeric esters (VEs) are one of the most promising biofuels. To investigate the feasibility of bimetallic Nb-Cu/ZPS as an esterification catalyst, direct conversion of LA was examined for the production of VEs over 4Nb-40Cu/ZPS in various C1–C5 alcohols at 150 °C using a catalyst-to-feed ratio of 0.125 for a reaction time of 2 h (Fig. S12a). As the chain length of the alcohols increased from C1 to C5, the LA conversion decreased from 80.5% to 30.2%, and the yield towards the VEs decreased scientifically from 67.4% to 0.1%. The higher LA conversion and VE selectivity achieved with the use of short-chain alcohols may be due to the strong polarity of these solvents (which facilitates proton liberation) and their lower steric hindrance compared to that of their long-chain counterparts. After finding these results, VA was directly converted over 4Nb-40Cu/ZPS in various C1–C5 alcohols at 150 °C and a catalyst-to-feed ratio of 0.125 for 2 h. Fig. S12b shows the VA conversion and selectivity of the corresponding valerate esters in the various alcoholic media. The Brønsted acid sites of the bimetallic Nb-Cu/ZPS catalyst facilitated the esterification reaction.¹³ As the chain length of the alcohols increased from C1 to C5, the VA conversion decreased from 98.0% to 91.0%, and the selectivity towards the VEs decreased from 100% to 88.0%. A similar trend was observed in previous reports.^{14, 15} Therefore, the bimetallic Nb-Cu/ZPS catalysts can be used for the direct conversion of LA to VA, as well as for the production of VE from VA in high yields when methanol was used as the solvent and reactant.

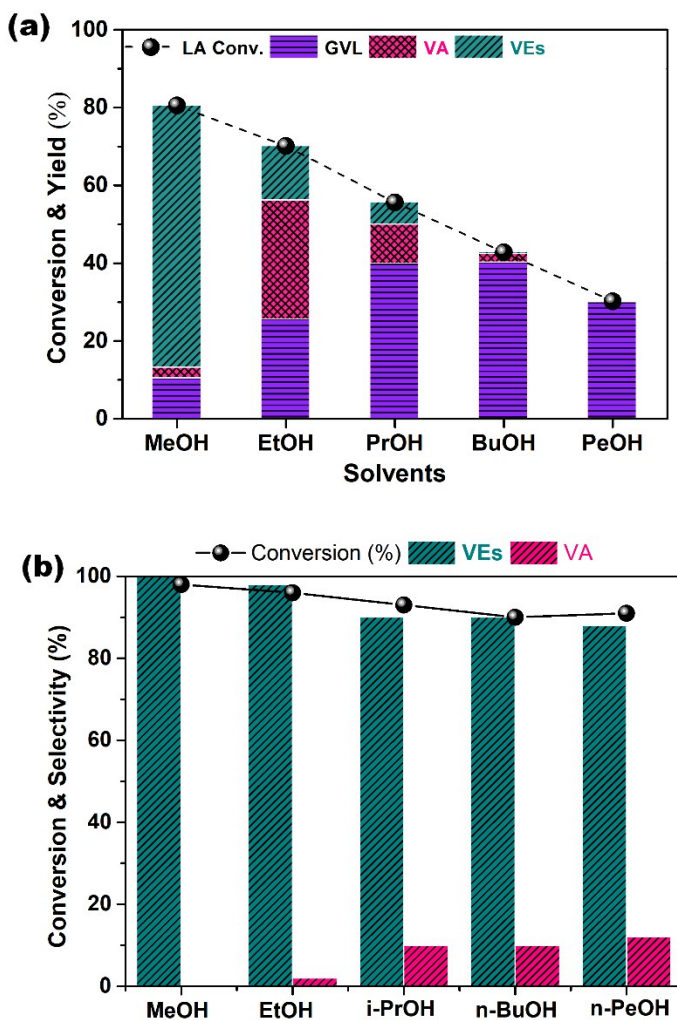


Fig. S12 (a) LA conversion and yields of various valeric esters (VEs) over 4Nb-40Cu/ZPS catalyst. Reaction conditions: 3.4 mmol LA, 30 mL alcohols, 3 MPa initial H₂ pressure, 150 °C, 2 h, (b) VA conversion and yields of various valeric esters (VEs) over 4Nb-40Cu/ZPS catalyst. Reaction conditions: 3.4 mmol VA, 30 mL H₂O, 3 MPa initial H₂ pressure, 150 °C, 2 h.



Fig. S13 Photographs of fresh, spent, and re-activated catalysts showing color changes. Re-activation conditions: 500 °C, 4 h, 5% H₂/Ar at flow rate of 30 mL min⁻¹.

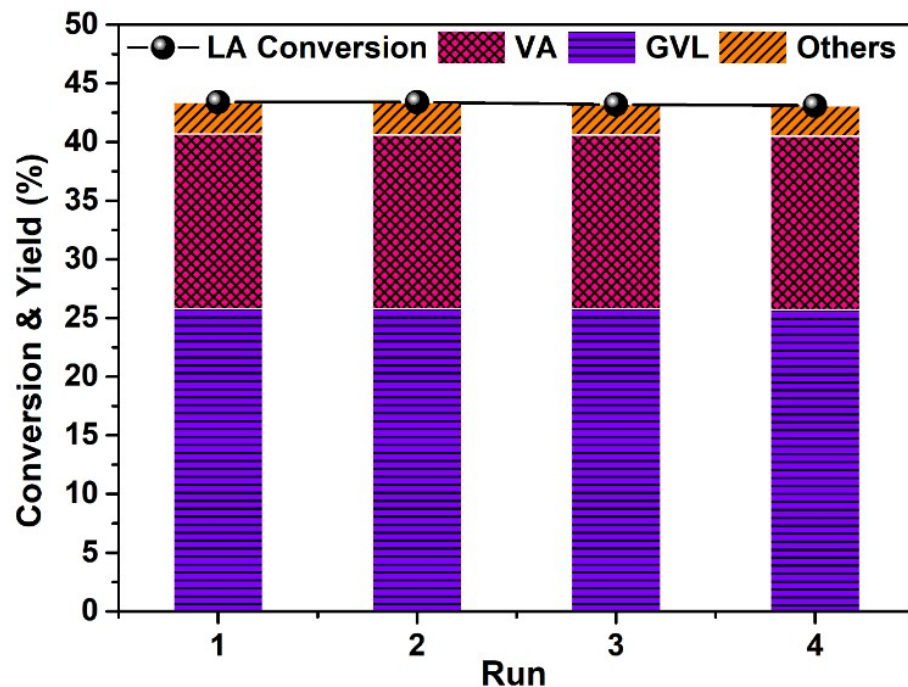


Fig. S14 Evaluation of intrinsic properties 4Nb-40Cu/ZPS catalyst by reuse in the conversion of LA under low conversion conditions. Reaction conditions: 3.4 mmol LA, 0.05 g catalyst, 40 mL H₂O, 120 °C, 3 MPa initial H₂ pressure, 1 h.

Kinetics of LA conversion and VA selectivity over the Cu/ZPS and Nb-Cu/ZPS catalysts

LA conversion followed first order reaction kinetics

$$\frac{dC_{LA}}{dt} = -kC_{LA}$$

By integrating the equation over time, then

$$C_{LA(t)} = C_{LA(0)}e^{-kt}$$

$$\frac{C_{LA(t)}}{C_{LA(0)}} = e^{-kt} \quad \frac{C_{LA(t)}}{C_{LA(0)}} = 1 - X_{LA}$$

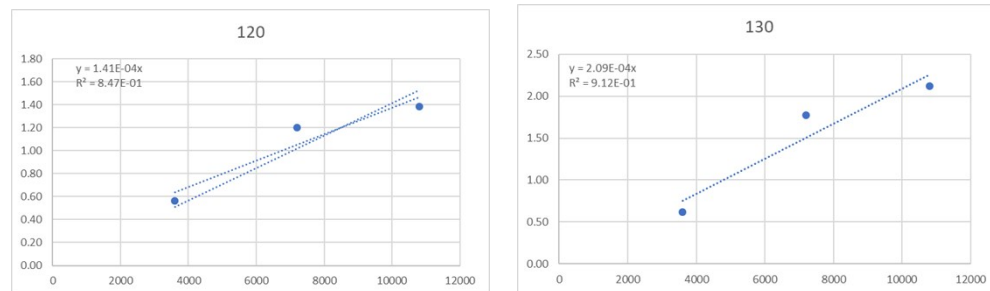
$$1 - X_{LA} = e^{-kt} \quad -\ln(1 - X_{LA}) = kt$$

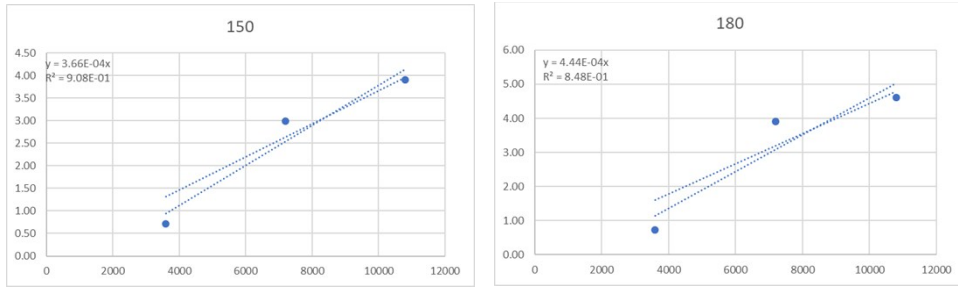
Plot = LA conversion vs time and obtained rate constant.

Temperature (°C)	Time (s)	X _{LA} ^a (mmol)	1-X _{LA}	Ln(1-X _{LA})	-Ln(1-X _{LA})
120	3600	0.43	0.57	-0.56	0.56
120	7200	0.7	0.3	-1.2	1.2
120	10800	0.75	0.25	-1.39	1.39
130	3600	0.46	0.54	-0.62	0.62
130	7200	0.83	0.17	-1.77	1.77
130	10800	0.88	0.12	-2.12	2.12
150	3600	0.51	0.49	-0.71	0.71
150	7200	0.95	0.05	-3	3
150	10800	0.98	0.02	-3.91	3.91
180	3600	0.52	0.48	-0.73	0.73
180	7200	0.98	0.02	-3.91	3.91
180	10800	0.99	0.01	-4.61	4.61

Reaction Conditions: 3.4 mmol of LA, 0.05 g of catalyst, 30 mL of H₂O, initial H₂ pressure of 3 MPa.

^aConversion of LA





T (°C)	1/T (kelvin)	Rate constant (k)	ln k
120	0.00254	1.41E-04	-8.86
130	0.00248	2.09E-04	-8.47
150	0.00236	3.66E-04	-7.91
180	0.00221	4.40E-04	-7.73

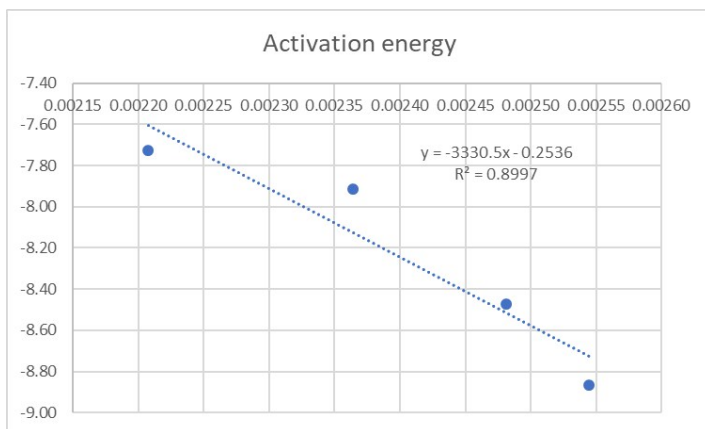
Calculate the activation energy (E_a) using Arrhenius equation

$$k = A \exp\left(-\frac{E_a}{R.T}\right) \quad \ln k = -\frac{E_a}{R.T} + \ln A$$

$$\ln k = -\frac{E_a}{R.T} + \ln A$$

Plot 1/T vs ln k (120–180 °C) $y = mx + C$

Slope = $-E_a/R \rightarrow$ Obtain E_a



Slope = 3330.5, $R = 0.008314 \text{ MPa L/mol.K}$

$E_a = 27.689 \text{ KJ/mol}$

Table S2 Reaction data of various catalyst used for kinetic energy calculation

Temperature	Time (s)	X _{LA} ^a (mmol)		Y _{PA} ^b (mmol)		
		2Nb- 40Cu/ZPS	40 Cu/ZPS	2Nb- 40Cu/ZPS	4Nb- 40Cu/ZPS	6Nb- 40Cu/ZPS
120	3600	0.3	0.11	0.11	0.149	0.141
	7200	0.57	0.25	0.21	0.507	0.39
	10800	0.58	0.27	0.23	0.658	0.42
130	3600	0.32	0.16	0.135	0.16	0.156
	7200	0.6	0.35	0.25	0.692	0.47
	10800	0.61	0.37	0.28	0.72	0.51
150	3600	0.4	0.35	0.16	0.185	0.177
	7200	0.87	0.803	0.45	0.745	0.701
	10800	0.89	0.86	0.65	0.846	0.812
180	3600	0.46	0.44	0.189	0.215	0.3
	7200	0.95	0.87	0.506	0.925	0.83
	10800	0.98	0.95	0.7	0.958	0.89

Reaction Conditions: 3.4 mmol of LA, 0.05 g of catalyst, 30 mL of H₂O, initial H₂ pressure of 3 MPa.

^aConversion of LA

^byield of LA

References

1. W. Luo, U. Deka, A. M. Beale, E. R. van Eck, P. C. Bruijnincx and B. M. Weckhuysen, *J. Catal.*, 2013, **301**, 175-186.
2. T. Pan, J. Deng, Q. Xu, Y. Xu, Q. X. Guo and Y. Fu, *Green Chem.*, 2013, **15**, 2967-2974.
3. W. Luo, P. C. Bruijnincx and B. M. Weckhuysen, *J. Catal.*, 2014, **320**, 33-41.
4. K. Kon, W. Onodera and K. i. Shimizu, *Catal. Sci. Technol.*, 2014, **4**, 3227-3234.
5. J. Zhou, R. Zhu, J. Deng and Y. Fu, *Green Chem.*, 2018, **20**, 3974-3980.
6. A. Wang, Y. Lu, Z. Yi, A. Ejaz, K. Hu, L. Zhang and K. Yan, *ChemistrySelect*, 2018, **3**, 1097-1101.
7. X. m. Gu, B. Zhang, H. j. Liang, H. b. GE, H. m. Yang and Q. Yong, *J. Fuel Chem. Technol.*, 2017, **45**, 714-722.
8. J. P. Lange, R. Price, P. M. Ayoub, J. Louis, L. Petrus, L. Clarke and H. Gosselink, *Angew. Chem. Int. Ed.*, 2010, **49**, 4479-4483.
9. P. Sun, G. Gao, Z. Zhao, C. Xia and F. Li, *ACS Catal.*, 2014, **4**, 4136-4142.
10. P. Sun, G. Gao, Z. Zhao, C. Xia and F. Li, *Appl. Catal., B*, 2016, **189**, 19-25.
11. V. V. Kumar, G. Naresh, S. Deepa, P. G. Bhavani, M. Nagaraju, M. Sudhakar, K. Chary, J. Tardio, S. Bhargava and A. Venugopal, *Appl. Catal., A*, 2017, **531**, 169-176.
12. V. K. Velisoju, N. Gutta, J. Tardio, S. K. Bhargava, K. Vankudoth, A. Chatla, S. Medak and V. Akula, *Appl. Catal., A*, 2018, **550**, 142-150.
13. I. A. Bassan, D. R. Nascimento, R. A. San Gil, M. I. P. da Silva, C. R. Moreira, W. A. Gonzalez, A. C. Faro Jr, T. Onfroy and E. R. Lachter, *Fuel Process. Technol.*, 2013, **106**, 619-624.
14. P. Sun, G. Gao, Z. Zhao, C. Xia and F. Li, *ACS Catal.*, 2014, **4**, 4136-4142.
15. K. Kon, W. Onodera and K. i. Shimizu, *Catal. Sci. Technol.*, 2014, **4**, 3227-3234.